Supplementary information

Deep eutectic solvent-based microextraction system for simultaneous lignocellulose fractionation and furfural production

Liu Liu, Qianwei Li, Caixia Wan*

Department of Chemical and Biomedical Engineering, University of Missouri, 1406 Rollins Street, Columbia, MO, United States 65211

* Corresponding author: Tel: +1 573 884 7882, Email: wanca@missouri.edu

Numbers of Page: 15

Number of Table: 8

Number of Figure: 3

Quantitative analysis

Quantitative analysis was performed according to the method described by Wen et al.[1]

$$I_{C9} = I(S_{2/6} + S'_{2/6})/2 + I(G_2) + I(H_{2/6})/2 \quad \text{(S1)}$$

where I_{C9} represents the integral value of aromatic ring in lignin; $I(S_{2,6}+S'_{2/6})$ is the integration of $S_{2/6}$ and $S'_{2/6}$; $I(G_2)$ is the integral value of G_2; $I(H_{2/6})$ is the integral value of $H_{2,6}$. The integration was conducted in the same contour level by using MestReNova.

$$I_X\% = I_X/I_{C9} \times 100\% \quad \text{(S2)}$$

where I_X is the integral value of A (β–O–4, β'–O–4), B (β–5), and C (β–β); S/G ratio was calculated with the following equation:

$$\text{S/G ratio} = I(S_{2/6} + S'_{2/6})/2/I(G_2) \quad \text{(S3)}$$

Enzymatic hydrolysis

The enzymatic hydrolysis was carried out at 50 °C for 72 h in an incubator shaker. The pretreated solids (2 g) were added to 20 mL of citric acid buffer (50 mM, pH 5.5) and NaN_3 was then added to the mixture.

The enzyme loading was 5 mg protein/g solid, with Cellic® CTec2 and HTec2 added at 10:1 volumetric mixing ratio. After the hydrolysis, the enzymes were deactivated by heating the mixture at 80 °C. The liquid was collected for sugar analysis using high performance liquid chromograph (HPLC). Glucose yields were calculated according to Equation S4.

$$Glucose\ yield\ (\%) = \frac{Mass\ of\ glucose\ released\ after\ hydrolysis}{Mass\ of\ cellulose\ \ in\ pulp} \times 0.9 \times 100\% \quad \text{(S4)}$$

Table S1. Composition of biphasic solvent systems

Sample No.	Aqueous phase (wt%)					Organic phase (wt%)
	DES (PEG:OA)	NaCl solution			H_2O	MIBK
		Total	NaCl	H_2O		
D_{70}	70.0	-	-	-	-	30.0
$D_{63}W_7$	63.0	-	-	-	7.0	30.0
$D_{49}W_{21}$	49.0	-	-	-	21.0	30.0
$D_{35}W_{35}$	35.0	-	-	-	35.0	30.0
$D_{56}S_{14}$	56.0	14.0	3.5	10.5	-	30.0
$D_{49}S_{21}$	49.0	21.0	5.3	15.7	-	30.0
$D_{42}S_{28}$	42.0	28.0	7.0	21.0	-	30.0
$D_{35}S_{35}$	35.0	35.0	8.8	26.2	-	30.0
$D_{28}S_{42}$	28.0	42.0	10.5	31.4	-	30.0
$D_{21}S_{49}$	21.0	49.0	12.3	36.7	-	30.0
$D_{14}S_{56}$	14.0	56.0	14.0	41.9	-	30.0

Table S2. Thermal behavior of DES with PEG mole fraction (χ_{PEG}) varied from 0.1 to 1

χ_{PEG}	Melting point (Tm, °C)	Melting enthalpy (ΔHm, J/g)
0.1	97.16	565.5
0.3	25.90	38.2
0.5	-63.94	5.0
0.7	-22.09	38.8
0.9	-13.11	105.7
1.0	-10.37	131.2

Table S3. Viscosity of DES

Sample [a]	Viscosity [mPa·s][b]
PEG 400	63.03
DES +0%H_2O	215.17
DES+10%H_2O	107.95
DES+20%H_2O	28.45
DES+40%H_2O	33.38

[a] In DES, molar ratio of PEG and OA was 1:1.
[b] Viscosity measured at room temperature.

Table S4. Xylose conversion under different reaction conditions

Sample No. of biphasic solvent	Reaction condition		Xylose conversion
	Temperature (°C)	Time (min)	(mol%)
$D_{56}S_{14}$	150	60	93.75±0.44
$D_{49}S_{21}$	150	60	97.33±0.33
$D_{42}S_{28}$	150	60	96.76±0.81
$D_{35}S_{35}$	150	60	98.23±1.10
$D_{28}S_{42}$	150	60	97.54±1.03
$D_{21}S_{49}$	150	60	94.19±0.77
$D_{14}S_{56}$	150	60	88.01±1.10
$D_{42}S_{28}$	160	60	99.92±0.06
$D_{42}S_{28}$	140	60	74.93±2.36
$D_{42}S_{28}$	130	60	50.46±0.01
$D_{42}S_{28}$	150	20	66.45±3.64
$D_{42}S_{28}$	150	40	92.20±2.62
$D_{42}S_{28}$	150	80	99.93±0.05
$D_{42}S_{28}$	150	100	100.00±0.01

Table S5. Structural characteristics of lignin by 2D HSQC NMR

Lignin type	Lignin interlinkage abundance (%) *			S/G ratio
	β-O-4	β-5	β-β	
PEG-g-lignin	18.25	0.37	2.44	1.47

* Data expressed as per 100 Ar.

Table S6. NaCl effect on acidity of DES (PEG:OA)

No.	DES (wt%)	25%NaCl solution (wt%)	H_2O (wt%)	pH	mV
1	80	20	-	0.68	368
2	60	40	-	0.45	381
3	40	60	-	0.30	390
4	20	80	-	0.16	397
5	80	-	20	1.48	324
6	60	-	40	1.44	326
7	40	-	60	1.45	325
8	20	-	80	1.60	317
9	100	0	-	1.19	340
10	0	100	-	6.52	43

Table S7. Comparison of furfural production via biphasic systems*

Feedstock	Biphasic system	Catalyst	Temperature (°C)	Duration (min)	Furfural yield (%)	Ref.
Xylose	SBP/H_2O	-	190	180	59	2
Birch hydrolysate liquor	SBP/H_2O	-	190	180	54	3
Xylose	EA/ChCl:H_2O:PTSA	-	130	15	50	3
Xylose	2-MTHF/NaCl solution	MC-SnO_x/NaCl	180	20	53.9	4
Xylose	MIBK/H_2O	$AlCl_3$/HCl	160	12	90	5
Xylose	Toluene/H_2O	H_2SO_4	190	2.5	70	6
Xylan	GVL/LiCl·3H_2O	LiCl·3H_2O	140	120	77.22	7
Corncob	Toluene/H_2O	$CrCl_3$·6H_2O/NaCl	140	60	23.88	8
Corn Stover	THF/H_2O	$AlCl_3$·6H_2O/NaCl	160	60	55	9
Switchgrass	THF/H_2O	$AlCl_3$·6H_2O/NaCl	160	60	56	10
Pinewood	THF/H_2O	$AlCl_3$·6H_2O/NaCl	160	60	38	10
Poplar	THF/H_2O	$AlCl_3$·6H_2O/NaCl	160	60	64	10
Corn Stalk	GVL/H_2O	[BMIM]Cl/$AlCl_3$	140	240	47.96	10
Eucalyptus	2-MTHF/ChCl:LA	$Al_2(SO_4)_3$/H_2SO_4	150	30	54.7	11
Bamboo	GVL/BDO:ChCl	$Al_2(SO_4)_3$/H_2SO_4	130	90	53.81	12
Corncob	MIBK/$FeCl_3$ solution	$FeCl_3$	180	60	73.49	13
Tung hull	MIBK/$FeCl_3$ solution	$FeCl_3$	180	60	69.38	14

Tung shell	MIBK/$FeCl_3$ solution	$FeCl_3$	180	60	99.86	[14]
Miscanthus×giganteus	MIBK/$FeCl_3$ solution	$FeCl_3$	180	60	73.75	[14]
Eucalyptus	MIBK/$FeCl_3$ solution	$FeCl_3$	180	60	75.18	[14]
Corncob	Toluene/H_2O	H_2SO_4	140	10	65.67	[14]
Corncob	DOP/ChCl:OA	$AlCl_3 \cdot 6H_2O/H_2SO_4$	120	30	46	[15]
Wheat straw	THF/NaCl solution	$CrPO_4$	180	90	67	[16]
Switchgrass	MIBK/PEG:OA	NaCl	150	60	76.5	This work

* 2-MTHF: 2-methyltetrahydrofuran; ChCl: Choline chloride; LA: Lactic acid; MIBK: Methyl isobutyl ketone; GVL: γ-valerolactone; BDO: 1,4-butanediol; DOP: Dioctyl phthalate; SBP: 2-sec-butylphenol; PTSA: *p*-toluenesulfonic acid; EA: Ethyl acetate; THF: Tetrahydrofuran toluene.

Table S8. Assignments of ATR-FTIR bands for pulp and switchgrass

	Wavenumber (cm^{-1})	Band assignments
Pulp	3346	v(O–H): cellulose, lignin
	1611, 1514	v(C=C): aromatic skeleton stretching of lignin
	1313	$\delta(CH_2)$ of crystalline cellulose: wagging; $\delta(CH_2)$: rocking
	1164	v_{as}(C–O–C): bridge of β–(1–4)–glycosidic in crystalline cellulose; v(C–O) of glucopyranose; v(C–O–C) of carbohydrate; δ(C–H) of carbohydrate
	1104	v(C–O): H–OOC– from OA, C–O from PEG
	1054	v(C–O): primary alcohol of carbohydrate; C–O– ether of cellulose or CH_3–O in lignin; CH_3–O– of ester and β–O–4 linkages in lignin
	777, 721	δ_{oop} (O–H) of crystalline cellulose
Switchgrass	3361	v(O–H): cellulose, lignin, hemicellulose
	1606, 1514	v(C=C): aromatic skeleton stretching of lignin
	1318	$\delta(CH_2)$ of crystalline cellulose: wagging; $\delta(CH_2)$: rocking
	1164	v_{as}(C–O–C): bridge of β–(1–4)–glycosidic in crystalline cellulose; v(C–O) of glucopyranose; v(C–O–C) of carbohydrate; δ(C-H) of carbohydrate
	1069	v(C–O): primary alcohol of carbohydrate; C–O– ether of cellulose or CH_3–O in lignin; CH_3–O– of ester and β–O–4 linkages in lignin
	986	δ_{oop} (C–H): Deformation in lignin

* v: stretching vibration; v_{as}: asymmetric stretching vibration; δ: in plane deformation; δ_{oop}: out-of-plane bending vibration

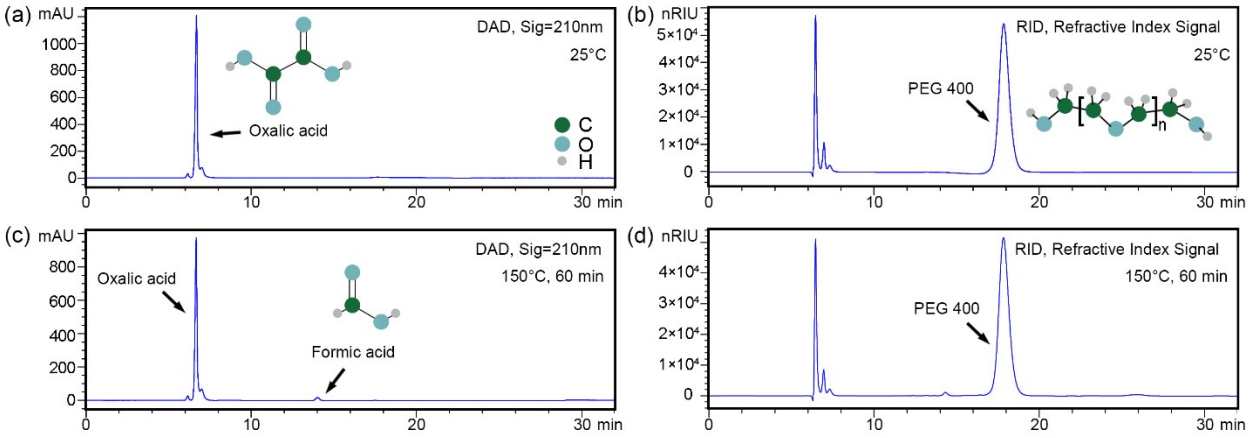

Figure S1. HPLC chromograms of the DES from $D_{42}S_{28}$ before (a, b) and after (c, d) heating at 150 °C for 60 min.

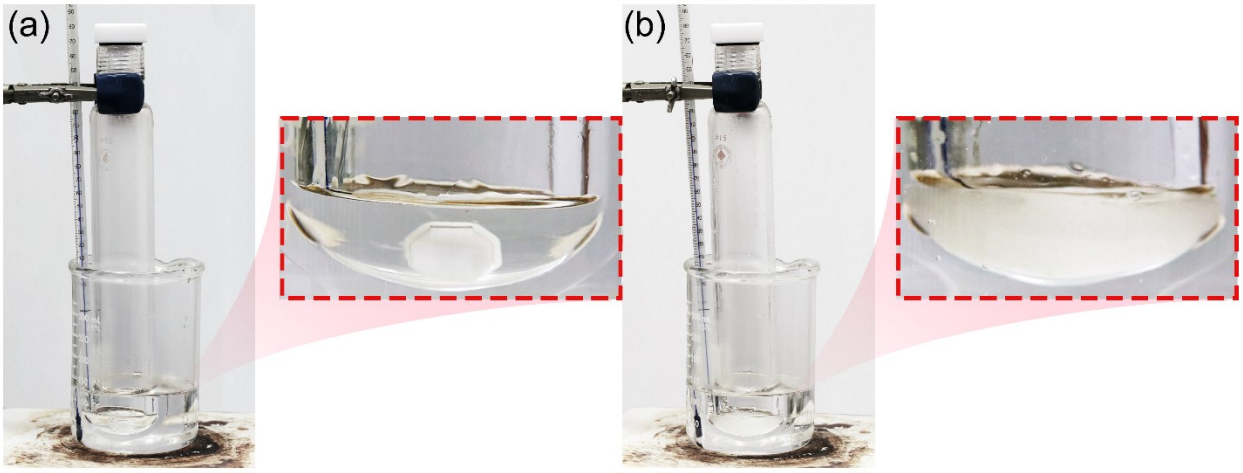

Figure S2. DES-based biphasic solvent at heating around 120 °C without (a) and with (b) NaCl solution. (120°C is the maximum limit of the pressure tube. These pictures are used to show the mixture state under heating and stirring.)

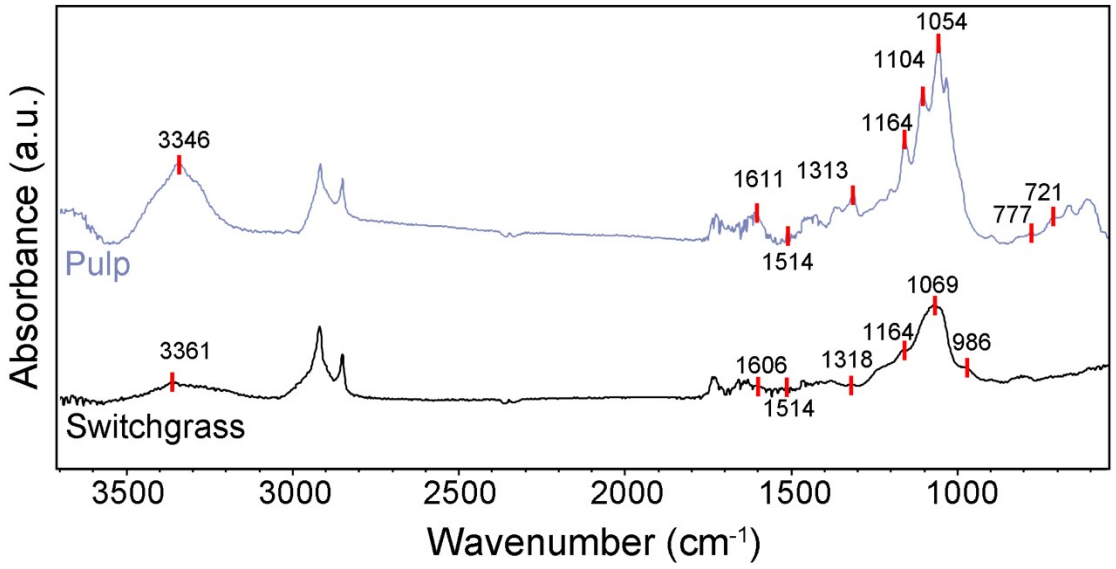

Figure S3. FTIR spectra of pulp (from $D_{42}S_{28}$) and switchgrass (assignments of bands in Table S8).

Reference

1. J.-L. Wen, B.-L. Xue, F. Xu and R.-C. Sun, *BioEnergy Research*, 2012, **5**, 886-903.
2. G. Gómez Millán, R. P. Bangalore Ashok, P. Oinas, J. Llorca and H. Sixta, *Biomass Conversion and Biorefinery*, 2021, **11**, 2095-2106.
3. D. M. E. Delgadillo, G. A. D. Castro and S. A. Fernandes, *Reaction Chemistry & Engineering*, 2024.
4. N. Zhou, C. Zhang, Y. Cao, J. Zhan, J. Fan, J. H. Clark and S. Zhang, *Journal of Cleaner Production*, 2021, **311**, 127780.
5. W. Guo, H. C. Bruining, H. J. Heeres and J. Yue, *Green Chemistry*, 2023, **25**, 5878-5898.
6. M. Papaioannou, R. J. T. Kleijwegt, J. van der Schaaf and M. F. Neira d'Angelo, *Industrial & Engineering Chemistry Research*, 2019, **58**, 16106-16115.
7. C. Liu, L. Wei, X. Yin, X. Pan, J. Hu, N. Li, J. Xu, J. Jiang and K. Wang, *Chemical Engineering Journal*, 2021, **425**, 130608.
8. Y. Zhang, M. Chen, J. Wang and Q. Hu, *Asian Journal of Chemistry*, 2014, **26**, 1717.
9. Y. Yang, C. W. Hu and M. M. Abu-Omar, *ChemSusChem*, 2012, **5**, 405-410.
10. S. Wang, Y. Zhao, H. Lin, J. Chen, L. Zhu and Z. Luo, *Green chemistry*, 2017, **19**, 3869-3879.
11. L.-L. Sun, Z. Yue, S.-C. Sun, S.-N. Sun, X.-F. Cao, T.-Q. Yuan and J.-L. Wen, *Bioresource Technology*, 2022, **352**, 127074.
12. J. Cheng, X. Liu, C. Huang, Y. Zhan, C. Huang, T. Chen, X. Meng, C. G. Yoo, G. Fang and A. J. Ragauskas, *Green Chemistry*, 2023, **25**, 6270-6281.
13. Q. Zhang, Z. Guo, X. Zeng, B. Ramarao and F. Xu, *Renewable Energy*, 2021, **179**, 351-358.
14. Q. Wang, W. Qi, W. Wang, Y. Zhang, N. Leksawasdi, X. Zhuang, Q. Yu and Z. Yuan, *Renewable Energy*, 2019, **144**, 139-146.
15. C.-Y. Bu, Y.-X. Yan, L.-H. Zou, S.-P. Ouyang, Z.-J. Zheng and J. Ouyang, *Bioresource Technology*, 2021, **319**, 124156.
16. Z. Cao, Z. Fan, Y. Chen, M. Li, T. Shen, C. Zhu and H. Ying, *Applied Catalysis B: Environmental*, 2019, **244**, 170-177.